SCIENCE CHINA
Chemistry

•ARTICLES•

March 2021 Vol.64 No.3: 445–451
https://doi.org/10.1007/s11426-020-9907-9

The initial attempt to reveal the emission processes of both mechanoluminescence and room temperature phosphorescence with the aid of circular dichroism in solid state

Yu Tian[1], Xuekang Yang[4], Yanbin Gong[2], Yunsheng Wang[1], Manman Fang[1*], Jie Yang[1], Zhiyong Tang[4] & Zhen Li[1,2,3*]

[1]*Institute of Molecular Aggregation Science, Tianjin University, Tianjin 300072, China;*
[2]*Department of Chemistry, Wuhan University, Wuhan 430072, China;*
[3]*Joint School of National University of Singapore and Tianjin University, International Campus of Tianjin University, Binhai New City, Fuzhou 350207, China;*
[4]*CAS Key Laboratory of Nanosystem and Hierarchical Fabrication, CAS Center for Excellence in Nanoscience, National Center for Nanoscience and Technology, Beijing 100190, China*

Received September 25, 2020; accepted November 9, 2020; published online January 11, 2021

A phenothiazine derivative **PtzChol** containing non-conjugated chiral cholesterol group was designed and synthesized. By analyzing the single crystal structure of **PtzChol** carefully, coupled with the circular dichroism (CD) signals before and after grinding, it was found that the introduction of cholesterol produced a positive effect on the production of chiral space group, on mechanoluminescence (ML) and room temperature phosphorescence (RTP), and throughout the entire light-emitting process, the CD signal could well reflect the changes of molecular arrangement.

mechanoluminescence, room temperature phosphorescence, circular dichroism, phenothiazine, cholesterol

Citation: Tian Y, Yang X, Gong Y, Wang Y, Fang M, Yang J, Tang Z, Li Z. The initial attempt to reveal the emission processes of both mechanoluminescence and room temperature phosphorescence with the aid of circular dichroism in solid state. *Sci China Chem*, 2021, 64: 445–451, https://doi.org/10.1007/s11426-020-9907-9

1 Introduction

Mechanoluminescence (ML), also known as triboluminescence (TL), represents one of the most interesting and least understood luminescence phenomena. It can be excited by grinding, rubbing, cutting, cleaving, shaking, scratching, compressing, or crushing of solids [1,2]. As a new light source, mechanoluminescence has attracted increasing attention and research interest of scientists, a wide range of applications not only in the field of intelligent pressure or crack sensing, but also in biological imaging, as light sources for phototherapy, magneto-optical sensing energy collection and displays [3–15]. As another special emission behavior, room temperature phosphorescence (RTP) of purely organic compounds, emitting from the transition forbidden triplet state, also has great potential in the applications of optoelectronic devices, bio-imaging and anti-counterfeiting due to its unique luminous advantages, such as long emission lifetime, and large Stokes shift [16–27]. So far, purely organic luminogens with both ML and RTP effects have been rarely reported, mainly for their unclear internal mechanisms and lacking of corresponding molecular design strategy, regardless of their importance for understanding complex luminescence processes and the relationship between the structural and optical properties [28–31]. Especially for mechanoluminescence, although the phenomenon can be

*Corresponding authors (email: manmanfang@tju.edu.cn; lizhentju@tju.edu.cn)

traced back hundreds of years ago, it has been slowly developed due to the lack of credible mechanisms and standard research methods [32–34]. Therefore, research on the mechanism of mechanoluminescence is bound to be the focus of research work, and thus, many research methods are required for the deep exploring.

According to previous researches, the molecular packing has played the important role in the luminescent properties and corresponding internal mechanisms. At present, the main methods for studying molecular packing are limited to single crystal X-ray diffraction and powder X-ray diffraction (PXRD) (Figure 1) [3–5,35]. Among them, single crystal X-ray diffraction could clearly present the molecular arrangement, but it requires the tested sample to be in a very good crystal state, while the powder one can just provide limited information and tedious data analyses are needed. As one of the most typical examples, ultraviolet-visible (UV-Vis) absorption spectrum is carried out to monitor the *H*/*J* aggregation in solid state. The forms of aggregation could well correspond to their emission behaviors, as the *J*-aggregation often leads to the brighter and red-shifted emission, while *H*-aggregation is not [17,36–42]. Similarly, circular dichroism (CD), as another relatively simple mean of monitoring the degree of molecular crystallinity, has also been applied to the field of photoelectronic properties closely related to molecular accumulation.

With this consideration in mind, we believe that the introduction of non-conjugated chiral elements into luminogens and monitoring the CD signal in solid state should be a good choice. First, the assembled chiral signal namely aggregation-induced circular dichroism (AICD) property can be easily detected in the UV-Vis light region, since non-conjugated chiral elements often transfer chirality to the entire molecule or the entire macroscopic system during the molecular assembly or packing process [43–48]; Secondly, the chiral elements will easily produce chiral molecular arrangement and piezoelectric effect in solid state, thus often leading to mechanoluminescence [49]; Thirdly, the regular molecular arrangement resulting from the chiral elements can contribute a lot to the rigid environment [50–54], then promoting the ML and RTP emissions. As we all know, phenothiazine has been widely reported as a good RTP building block, as the existence of N and S heteroatoms in it can largely promote the intersystem crossing and the resultant RTP emission [20,55]. In addition, it is not negligible that the conformation of *N*-aryl phenothiazine derivatives affects emission. Molecules with equatorial geometry often show red-shifted luminescence and stronger luminous efficiency, and are excellent dual-emitters. It is because the change of conformation not only affects the degree of conjugation and charge transfer of molecules, but also affects the packing modes of molecules [56–60]. Therefore, accordingly, in this work, the non-conjugated chiral group of cholesterol is combined with a typical RTP/ML building block of phenothiazine to yield **PtzChol**, with an attempt to introduce chiral element into solid sample with ML and RTP effects (Figure 1). Experimental data demonstrates that **PtzChol** crystal presents a chiral molecular packing, which is heavily related to its ML and RTP effects. Thus, through monitoring the changed CD signals in different states, the relationship between the molecular packing and luminescence could be well established accordingly.

2 Experimental

Experimental procedures and photophysical properties of **PtzChol** or **PtzMe**, crystal data, theoretical calculations, nuclear magnetic resonance (NMR) spectra and high resolution mass spectrometry (HRMS) spectra are listed in the Supporting Information online.

3 Results and discussion

The target compound of **PtzChol** was easily synthesized by esterification reaction (Scheme S1, Supporting Information online), and its structure has been well certified by ^{1}H NMR, ^{13}C NMR, and HRMS. To better understand the important role of chiral group, **PtzMe** was synthesized for comparison, in which the chiral group of cholesterol was replaced by methyl one (Scheme S2). Then their single crystals were obtained from a mixture solvent of dichloromethane (DCM) and petroleum ether (PE) (the volume ratio is 1:3) by solvent evaporation. Fortunately, dual emissions of fluorescence and phosphorescence could be clearly observed at room temperature for **PtzChol** crystal, while only fluorescence in **PtzMe** one. Also, when the mechanical stimulation, such as rubbing or crushing, was applied to **PtzChol** crystal, bright green emission could occur without any UV irradiation, totally opposite to that of **PtzMe**. Thus, through simply changing the substituent group from non-chiral methyl to chiral cholesterol, much different RTP and ML effects could be realized in these two compounds.

In order to figure out the origin of the different RTP and ML effects for these two compounds, their photophysical properties in solution state were first studied. As shown in Figure S1 (Supporting Information online), in dilute tetrahydrofuran (THF) solution, **PtzChol** and **PtzMe** gave similar UV-Vis absorption spectra with maximum absorption peaks at about 310 nm. Besides, their PL emission peaks both located around 535 nm at room temperature with the corresponding emission lifetimes measured to be 4.81 and 4.66 ns, respectively (Figures S2 and S3), indicating they were fluorescence. When their THF solutions were cooled to 77 K, similar PL spectra could also be recorded, although

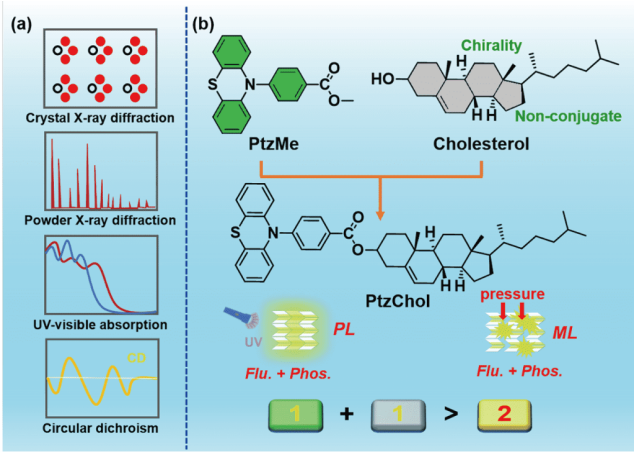

Figure 1 (a) Some methods and assumption for detecting molecular packing; (b) the design idea and the dual emission properties of compound **PtzChol** at room temperature (color online).

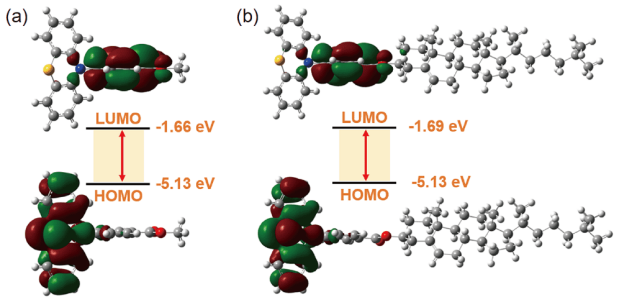

Figure 2 Frontier molecular orbitals. (a) HOMO, LUMO orbits and the corresponding energies of **PtzMe**; (b) HOMO, LUMO orbits and the corresponding energies of **PtzChol** (color online).

phosphorescence was dominated at this time for the restricted non-radiative motion (Figures S4 and S5). The consistency of their absorptions and emissions in dilute solutions indicated that these two luminogens presented the similar electronic structure and the introduction of non-conjugated chiral cholesterol group had nearly no influence on solutions. Also, their cyclic voltammetry (CV) curves were measured and the corresponding highest occupied molecular orbital (HOMO)/lowest unoccupied molecular orbital (LUMO) values were calculated to be −5.13/−1.69 eV and −5.13/−1.66 eV for **PtzChol** and **PtzMe**, respectively (Figure 2 and Figure S6), further certifying their similar electronic structure. Thus, it was believed that the packing mode, rather than the molecular electronic structure, should account for their different RTP and ML in solid state.

The emission behaviors of **PtzChol** and **PtzMe** in solid state were studied carefully (Figures S7–S11). In **PtzMe** crystal, no RTP/ML effect was observed, although dominated phosphorescence emission existed at 77 K for the restricted non-radiative transition. As for **PtzChol** crystal, dual emission peaks could be found under the 365 nm irradiation and its overall emission quantum yield was as large as 7.15%. There are both two emission components (τ_1=2.4 ns and τ_2=0.73 ms) in the PL decay curves of 467 and 492 nm for their large overlap, indicating the fluorescence-phosphorescence dual emissions for **PtzChol** crystal. When it was ground heavily, just fluorescence peak of 467 nm retains with lifetime of 3.2 ns. Obvious mechanoluminescence could be observed for **PtzChol** crystal, and the main emission peak located at 492 nm (Figure 3(a)), indicating the dominated mechanophosphorescence effect. This might be from the denser molecular packing under mechanical stimulus, which could further restrict non-radiative motion and contribute much to the emission of phosphorescence, just like that at 77 K (Figure S8). If **PtzChol** crystal was destroyed through heavily grinding, both RTP and ML emissions would disappear, indicating the significant role of the particular molecular packing in them. Then what kind of molecular packing should be responsible for these unique emission properties? Whether the chiral element has played a role in this process?

To answer these questions, the measurements of CD in solid state were carried out. As shown in Figure 3(c), strong signals could be observed in the CD absorption spectra of **PtzChol** crystal for different measurement angles, including 0°, 45°, 90°, and 135°, respectively, demonstrating the chiral molecular arrangement in crystal. Also, they were all in good agreement with each other, indicating the accuracy of CD signals. However, if **PtzChol** crystal was ground heavily, its CD signals would nearly disappear due to the destroyed molecular arrangement, indicating that CD could be just achieved through the regular molecular packing. Unfortunately, the circularly polarized luminescence (CPL) signal has not been detected.

To further confirm that CD signals were derived from the chiral molecular arrangement rather than chiral molecular structure, the CD absorption spectrum in solution was measured (Figure S12). No CD signal could be detected for **PtzChol** solution, and thus, the similar changed tendency between chiral molecular arrangement and ML/RTP effect could be certified, showing their potential relationship.

In order to further investigate the effect of chiral element on the molecular arrangement and luminescence properties, the single crystal structures of **PtzChol** and **PtzMe** were analyzed carefully. Owing to the introduction of chiral cholesterol group, **PtzChol** crystal presented the *C*2 chiral space group, in which the strong CD signals could be realized. Furthermore, because of the non-central symmetric effect of chiral space group, the piezoelectric effect was easy to be achieved, which has been thought to be the main origin for some ML phenomena. As for **PtzMe** with methyl substituent, the central-symmetric space group of $P2_1/n$ was observed (Table S1). Also, much stronger intermolecular interactions could be formed in **PtzChol** crystal with chiral molecular arrangement than that in **PtzMe**. In order to

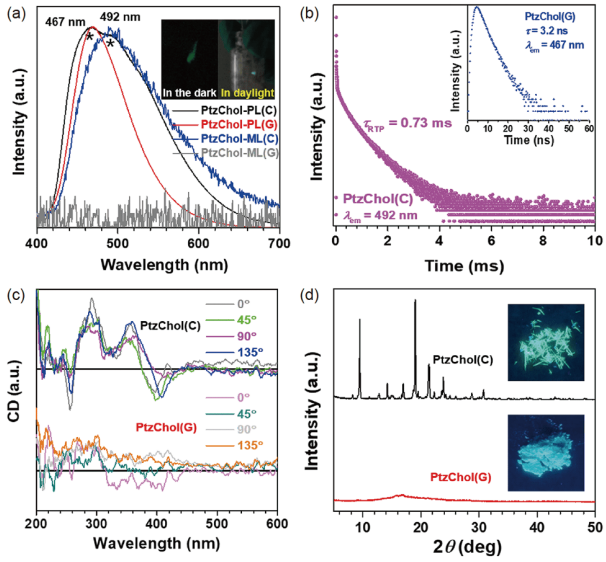

Figure 3 (a) Normalized PL and ML spectra of **PtzChol** in crystal (C) and ground (G) states at room temperature. Inset: ML image of **PtzChol** crystal upon grinding with a glass rod in daylight and the dark. (b) Time-resolved PL-decay curves for **PtzChol** in crystal and ground (inset) states, respectively. (c) CD absorption spectra of **PtzChol** in crystal and ground states measured from different angles. (d) The PXRD patterns for **PtzChol** in crystal and ground states (color online).

simplify the packing analyses and make a clear description, dimers based on two adjacent molecules with strong intermolecular interactions were selected and listed. As shown in Figure 4(c), five kinds of molecular dimers could be found in **PtzChol** crystal, in which dimer 1 was coupled with two efficient C–H···C interactions (3.10 Å), dimer 2 with C–H···C (3.11 Å) bond, dimer 3 with four kinds of interactions, including C–H···O (2.81 Å), C–H···π (3.22 Å), C–H···S (3.11 Å) and π···π (3.70 Å) interactions; dimer 4 with C–H···O (3.50 Å), C–H···π (2.82 Å), C–H···C (2.81, 2.98, 3.14 and 3.22 Å) bonds; dimer 5 with C–H···O (2.76 Å), C–H···π (2.95, 3.22 Å), C–H···S (2.92 Å) and C–H···C (3.01, 3.07 and 3.09 Å) bonds. All these intermolecular interactions could contribute a lot to the restricted non-radiative motion, thus promoting the RTP and ML emissions. As for **PtzMe** crystal, much weaker intermolecular interactions were found, including C–H···O (2.65, 2.65, 2.48 Å), π···π (3.49 Å) and C–H···π (2.62, 2.88, 2.99, 3.06, 3.28, 3.24 and 3.51 Å) interactions (Figure S13).

Moreover, theoretical calculations were carried out to evaluate the influence of chiral molecular arrangement on ML and RTP emissions. First, the dipole moments of their single molecules and dimers were calculated. In the single molecule state, **PtzChol** and **PtzMe** presented the similar dipole moments of 3.26 and 2.45 D (1 D=3.33564×10^{-30} C m), respectively (Figure 4(b) and Figure S13(a)), for their similar electronic structures. However, for the dimers of **PtzChol**, selected from the chiral molecular arrangement, their dipole moments largely increased to 4.65, 4.53, 4.65, 6.23, and 5.89 D, respectively (Figure 4(c)). It was believed that these large dipole moments could promote the piezoelectric effect, as well as the ML emission in **PtzChol** crystal. As for the dimers in **PtzMe** crystal, most of dipole moments decreased to around 1 D for its central-symmetric space group. Thus, the calculated dipole moments in the molecular dimer well demonstrated the important role of chiral molecular arrangement in the ML emission.

Then the HOMO and LUMO orbital distributions for their single molecules and dimers were analyzed. In the single molecule state, the HOMOs mainly located on the part of phenothiazine, while the LUMOs were at methyl benzoate for both **PtzChol** and **PtzMe** (Figures S14 and S15). This further indicated the similar electronic structures of **PtzChol** and **PtzMe** in theory, and the non-conjugated chiral cholesterol group had little influence on it. As for their molecular dimers, selected from the single crystal structures, much different HOMO and LUMO orbital distributions were found for their different molecular arrangement. Particularly, efficient intermolecular charge transfer could be realized for dimers in **PtzChol**, from an occupied orbital of one molecule to a vacant orbital of a neighboring molecule (Figure 5). This could contribute much to the increased dipole moments. As for the dimers in **PtzMe** crystal, the charge transfers mainly occurred within one molecule (Figure S15). Thus, the intermolecular and intramolecular charge transfer in **PtzChol** and **PtzMe** could both contribute to their efficient intersystem crossing (ISC) transition as well as phosphorescence at low temperature, in which the non-radiative motion was restricted. When it turned to room temperature, the non-radiative motion would dominate in **PtzMe** crystal, and thus no RTP emission could be observed. As for **PtzChol** crystal, the much stronger intermolecular interactions, resulting from the regular chiral molecular arrangement, were still able to restrain intramolecular motion, thus resulting in the RTP emission.

In order to check the effect of oxygen on room temperature phosphorescence, the PL spectra of the product under deoxygenated state were measured. As shown in Figure S16, oxygen does have an effect on phosphorescence emission to a certain extent, but it is not a decisive factor, because the phosphorescence component of **PtzChol** exposed to the air is only weakened and does not disappear compared to the deoxidized state. And no phosphorescence of **PtzMe** in the deoxygenated state was detected. Therefore, these results further confirm the introduction of chiral cholesterol group as a key role in phosphorescence emission, as described above.

As revealed by our experimental results, coupled with the theoretical calculations, the chiral molecular arrangement played a significant role in the light-emitting process of **PtzChol**, including ML and RTP. In crystal, the introduction of chiral cholesterol group would lead to the regular chiral

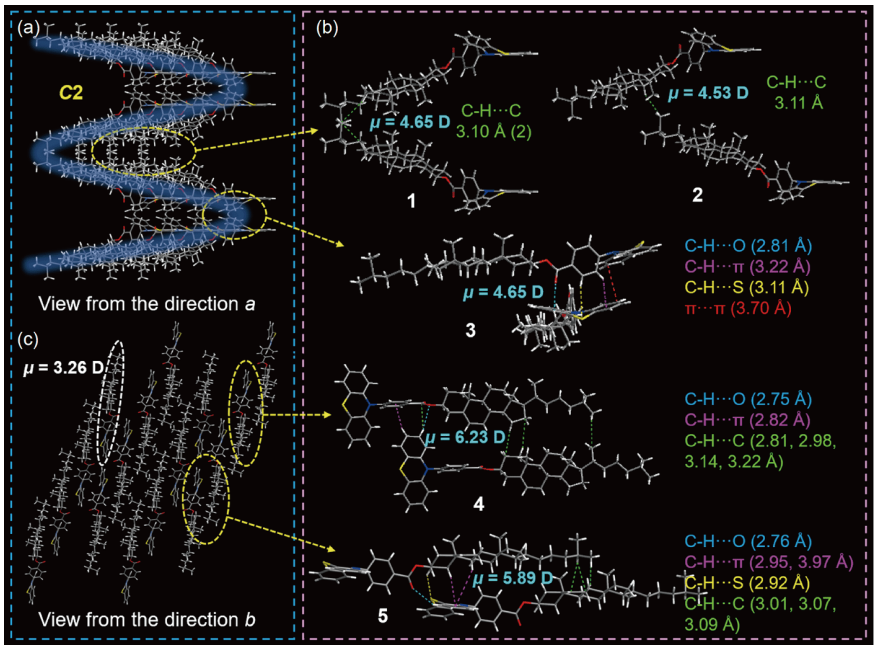

Figure 4 (a, b) Molecular packing of **PtzChol** crystal observed from *a* and *b* directions, respectively; (c) dimers of **PtzChol** crystal and their intermolecular interactions (color online).

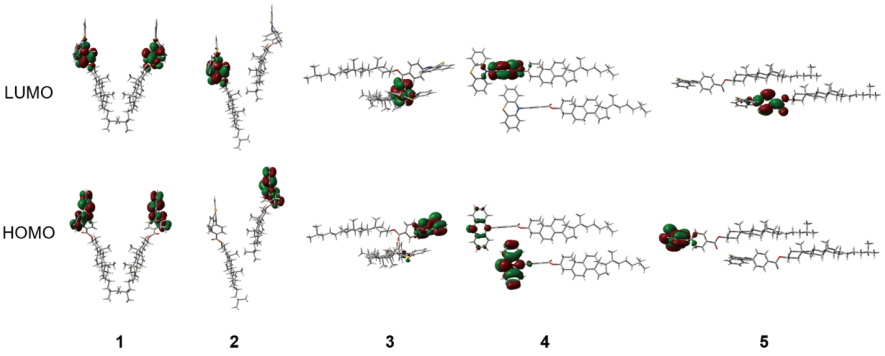

Figure 5 Dimer-based molecular frontier orbit. HOMO, LUMO orbits of five dimers in **PtzChol** (color online).

molecular arrangement as well as strong CD signal in crystal state, which could be much beneficial for the enhanced intermolecular interaction as well as rigid environment, thus promoting the RTP emission. On the other hand, the non-central symmetric effect of chiral space group would largely increase the dipole moment of molecular dimers in crystal. Thus, when the mechanical stimulus was applied to it, the piezoelectric effect and the corresponding ML emission were easy to be achieved.

However, when the crystal was subjected to heavy grinding for a long time, the packing would become disordered, accompanying with the disappeared CD signal. At this time, the properties of ML and RTP both disappeared for severe destruction of chiral molecular arrangement. Throughout the entire light-emitting process, the CD signal, instead of the common single crystal/PXRD, could well monitor the changes of molecular arrangement (Figure 6).

4 Conclusions

We designed and synthesized a chiral molecule of **PtzChol** with both ML and RTP characters for the first time. Owing to the inductive effect of chiral cholesterol group, **PtzChol** crystal presented the *C*2 chiral space group, in which the strong CD signals could be realized. Furthermore, because of the non-central symmetric effect of chiral space group, the piezoelectric effect was easy to be achieved, which has been thought to be the main origin for some ML phenomena. Introduction of cholesterol can increase intermolecular forces, which could contribute a lot to the restricted non-radiative motion, thus promoting the RTP and ML emissions.

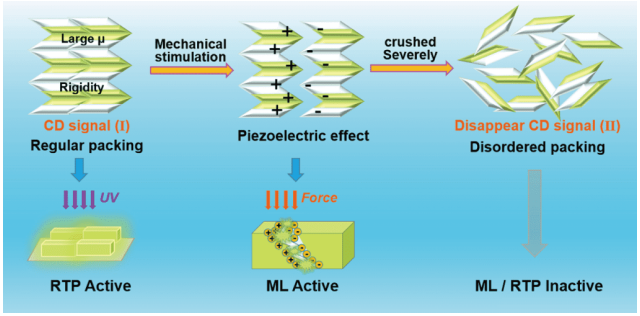

Figure 6 The proposed relationship between regular chiral molecular arrangement and ML/RTP effect (color online).

Strong CD signal could be observed in crystal state for the regular molecular packing, while nearly disappeared after heavy grinding. Thus, throughout the entire light-emitting process, the CD signal could well reflect the changes of molecular arrangement. Therefore, this work may have a positive effect on the design of molecules with ML and RTP, and prompt to explore new approaches to investigate the Molecular Uniting Set Identified Characteristc (MUSIC) [20,61–65].

Acknowledgements This work was supported by the National Natural Science Foundation of China (21905197), and the Starting Grants of Tianjin University and Tianjin Government.

Conflict of interest The authors declare no conflict of interest.

Supporting information The supporting information is available online at http://chem.scichina.com and http://link.springer.com/journal/11426. The supporting materials are published as submitted, without typesetting or editing. The responsibility for scientific accuracy and content remains entirely with the authors.

1 Walton AJ. *Adv Phys*, 1977, 26: 887–948
2 Zink JI. *Acc Chem Res*, 1978, 11: 289–295
3 Xie Y, Li Z. *Chem*, 2018, 4: 943–971
4 Xie Y, Li Z. *Mater Chem Front*, 2020, 4: 317–331
5 Mukherjee S, Thilagar P. *Angew Chem Int Ed*, 2019, 58: 7922–7932
6 Xu CN, Watanabe T, Akiyama M, Zheng XG. *Appl Phys Lett*, 1999, 74: 2414–2416
7 Terasaki N, Zhang H, Yamada H, Xu CN. *Chem Commun*, 2011, 47: 8034–8036
8 Wang X, Zhang H, Yu R, Dong L, Peng D, Zhang A, Zhang Y, Liu H, Pan C, Wang ZL. *Adv Mater*, 2015, 27: 2324–2331
9 Terasaki N, Yamada H, Xu CN. *Catal Today*, 2013, 201: 203–208
10 Mei J, Leung NLC, Kwok RTK, Lam JWY, Tang BZ. *Chem Rev*, 2015, 115: 11718–11940
11 Xu S, Liu T, Mu Y, Wang YF, Chi Z, Lo CC, Liu S, Zhang Y, Lien A, Xu J. *Angew Chem Int Ed*, 2015, 54: 874–878
12 Wang C, Xu B, Li M, Chi Z, Xie Y, Li Q, Li Z. *Mater Horiz*, 2016, 3: 220–225
13 Li W, Huang Q, Mao Z, Li Q, Jiang L, Xie Z, Xu R, Yang Z, Zhao J, Yu T, Zhang Y, Aldred MP, Chi Z. *Angew Chem Int Ed*, 2018, 57: 12727–12732
14 Wang C, Yu Y, Yuan Y, Ren C, Liao Q, Wang J, Chai Z, Li Q, Li Z. *Matter*, 2020, 2: 181–193
15 Li W, Huang Q, Mao Z, Li Q, Jiang L, Xie Z, Xu R, Yang Z, Zhao J, Yu T, Zhang Y, Aldred MP, Chi Z. *Angew Chem Int Ed*, 2018, 57: 12727–12732
16 Zhang T, Ma X, Wu H, Zhu L, Zhao Y, Tian H. *Angew Chem Int Ed*, 2020, 59: 11206–11216
17 An Z, Zheng C, Tao Y, Chen R, Shi H, Chen T, Wang Z, Li H, Deng R, Liu X, Huang W. *Nat Mater*, 2015, 14: 685–690
18 Wang J, Gu X, Ma H, Peng Q, Huang X, Zheng X, Sung SHP, Shan G, Lam JWY, Shuai Z, Tang BZ. *Nat Commun*, 2018, 9: 2963
19 Xu S, Chen R, Zheng C, Huang W. *Adv Mater*, 2016, 28: 9920–9940
20 Yang J, Zhen X, Wang B, Gao X, Ren Z, Wang J, Xie Y, Li J, Peng Q, Pu K, Li Z. *Nat Commun*, 2018, 9: 840
21 Zhao W, Cheung TS, Jiang N, Huang W, Lam JWY, Zhang X, He Z, Tang BZ. *Nat Commun*, 2019, 10: 1595
22 Zhao W, He Z, Lam JWY, Peng Q, Ma H, Shuai Z, Bai G, Hao J, Tang BZ. *Chem*, 2016, 1: 592–602
23 Xie Y, Ge Y, Peng Q, Li C, Li Q, Li Z. *Adv Mater*, 2017, 29: 1606829
24 Chen X, Xu C, Wang T, Zhou C, Du J, Wang Z, Xu H, Xie T, Bi G, Jiang J, Zhang X, Demas JN, Trindle CO, Luo Y, Zhang G. *Angew Chem Int Ed*, 2016, 55: 9872–9876
25 Cai S, Shi H, Zhang Z, Wang X, Ma H, Gan N, Wu Q, Cheng Z, Ling K, Gu M, Ma C, Gu L, An Z, Huang W. *Angew Chem Int Ed*, 2018, 57: 4005–4009
26 Fang M, Yang J, Xiang X, Xie Y, Dong Y, Peng Q, Li Q, Li Z. *Mater Chem Front*, 2018, 2: 2124–2129
27 Fang MM, Yang J, Li Z. *Chin J Polym Sci*, 2019, 37: 383–393
28 Yang J, Ren Z, Xie Z, Liu Y, Wang C, Xie Y, Peng Q, Xu B, Tian W, Zhang F, Chi Z, Li Q, Li Z. *Angew Chem Int Ed*, 2017, 56: 880–884
29 Yang J, Gao X, Xie Z, Gong Y, Fang M, Peng Q, Chi Z, Li Z. *Angew Chem Int Ed*, 2017, 56: 15299–15303
30 Zhang K, Sun Q, Zhang Z, Tang L, Xie Z, Chi Z, Xue S, Zhang H, Yang W. *Chem Commun*, 2018, 54: 5225–5228
31 Huang Q, Mei X, Xie Z, Wu D, Yang S, Gong W, Chi Z, Lin Z, Ling Q. *J Mater Chem C*, 2019, 7: 2530–2534
32 Hurt CR, Mcavoy N, Bjorklund S, Filipescu N. *Nature*, 1966, 212: 179–180
33 Nishida J, Ohura H, Kita Y, Hasegawa H, Kawase T, Takada N, Sato H, Sei Y, Yamashita Y. *J Org Chem*, 2016, 81: 433–441
34 Chandra BP, Chandra VK, Jha P, Patel R, Shende SK, Thaker S, Baghel RN. *J Lumin*, 2012, 132: 2012–2022
35 Ubba E, Tao Y, Yang Z, Zhao J, Wang L, Chi Z. *Chem Asian J*, 2018, 13: 3106–3121
36 Spano FC. *Acc Chem Res*, 2010, 43: 429–439
37 Kasha M, Rawls HR, Ashraf El-Bayoumi M. *Pure Appl Chem*, 1965, 11: 371–392
38 Eisfeld A, Briggs JS. *Chem Phys*, 2002, 281: 61–70
39 Li Z. *Sci China Chem*, 2017, 60: 1107–1108
40 Yang J, Chi Z, Zhu W, Tang BZ, Li Z. *Sci China Chem*, 2019, 62: 1090–1098
41 Li Q, Li Z. *Sci China Mater*, 2020, 63: 177–184
42 Walczak PB, Eisfeld A, Briggs JS. *J Chem Phys*, 2008, 128: 044505
43 Yang D, Duan P, Liu M. *Angew Chem Int Ed*, 2018, 57: 9357–9361
44 Shang H, Ding Z, Shen Y, Yang B, Liu M, Jiang S. *Chem Sci*, 2020, 11: 2169–2174
45 Yu C, Xue M, Liu K, Wang G, Fang Y. *Langmuir*, 2014, 30: 1257–1265
46 Yu H, Lü Y, Chen X, Liu K, Fang Y. *Soft Matter*, 2014, 10: 9159–9166
47 Pescitelli G, Di Bari L, Berova N. *Chem Soc Rev*, 2014, 43: 5211–5233
48 Duan P, Cao H, Zhang L, Liu M. *Soft Matter*, 2014, 10: 5428–5448
49 Chen Y, Xu C, Xu B, Mao Z, Li JA, Yang Z, Peethani NR, Liu C, Shi G, Gu FL, Zhang Y, Chi Z. *Mater Chem Front*, 2019, 3: 1800–1806
50 Hirata S, Totani K, Zhang J, Yamashita T, Kaji H, Marder SR, Watanabe T, Adachi C. *Adv Funct Mater*, 2013, 23: 3386–3397
51 Song J, Wang M, Zhou X, Xiang H. *Chem Eur J*, 2018, 24: 7128–7132
52 Hirata S, Vacha M. *J Phys Chem Lett*, 2016, 7: 1539–1545
53 Liang X, Liu TT, Yan ZP, Zhou Y, Su J, Luo XF, Wu ZG, Wang Y,

Zheng YX, Zuo JL. *Angew Chem Int Ed*, 2019, 58: 17220–17225
54 Hirata S, Totani K, Kaji H, Vacha M, Watanabe T, Adachi C. *Adv Opt Mater*, 2013, 1: 438–442
55 Tian Y, Gong Y, Liao Q, Wang Y, Ren J, Fang M, Yang J, Li Z. *Cell Rep Phys Sci*, 2020, 1: 100052
56 Kitade T, Kitamura K, Kishimoto N. *Anal Sci*, 1996, 12: 439–441
57 Borowicz P, Herbich J, Kapturkiewicz A, Anulewicz-Ostrowska R, Nowacki J, Grampp G. *Phys Chem Chem Phys*, 2000, 2: 4275–4280
58 Nobuyasu RS, Ward JS, Gibson J, Laidlaw BA, Ren Z, Data P, Batsanov AS, Penfold TJ, Bryce MR, Dias FB. *J Mater Chem C*, 2019, 7: 6672–6684
59 Kukhta NA, Bryce MR. *Mater Horiz*, 2021, doi: 10.1039/d0mh01316a
60 Gierschner J, Behera SK, Park SY. *Angew Chem Int Ed*, 2020, doi: 10.1002/anie.202009789
61 Xu R, Wang K, Chen G, Yan W. *Natl Sci Rev*, 2019, 6: 191–194
62 Li Q, Li Z. *Adv Sci*, 2017, 4: 1600484
63 Li Q, Tang Y, Hu W, Li Z. *Small*, 2018, 14: 1801560
64 Wang Y, Yang J, Fang M, Yu Y, Zou B, Wang L, Tian Y, Cheng J, Tang BZ, Li Z. *Matter*, 2020, 3: 449–463
65 Li Q, Li Z. *Acc Chem Res*, 2020, 53: 962–973